

Experimental observation of coherent interaction between laser and erbium ions ensemble doped in fiber at sub 10 mK

Qi XI¹, Shihai WEI¹, Chenzhi YUAN¹, Xueying ZHANG¹, You WANG^{1,2},
Haizhi SONG^{1,2*}, Guangwei DENG^{1,5*}, Bo JING¹,
Daniel OBLAK⁴ & Qiang ZHOU^{1,3,5*}

¹*Institute of Fundamental and Frontier Sciences, University of Electronic Science and Technology of China, Chengdu 610054, China;*

²*Southwest Institute of Technical Physics, Chengdu 610041, China;*

³*School of Optoelectronic Science and Engineering, University of Electronic Science and Technology of China, Chengdu 610054, China;*

⁴*Institute for Quantum Science and Technology, Department of Physics & Astronomy, University of Calgary, Calgary, T2N 1N4, Canada;*

⁵*CAS Key Laboratory of Quantum Information, University of Science and Technology of China, Hefei 230026, China*

Received 23 May 2020/Accepted 10 June 2020/Published online 15 July 2020

Abstract Rare-earth ions doped in solid-state materials are considered promising candidates for quantum information applications, especially for photonic quantum memory. Among them, erbium ions doped in an optical fiber have attracted a lot of attentions due to their ability to provide efficient photon-atom interaction on a telecom-C band compatible transition. The coherent photon-atom interaction, which is crucial for quantum memory, has not yet been investigated for erbium ions doped in fiber at the temperature of sub 10 mK with the magnetic environment. In this paper, we experimentally observe optical nutation, which results from the coherent interaction between laser and erbium ions ensemble, in a piece of 9.5-m-long fiber with the erbium concentration of 200 ppm. We also extract the transition dipole moment from the results of optical nutation and further investigate its dependence on laser wavelength and magnetic field. A transition dipole moment of $(3.424 \pm 0.019) \times 10^{-32}$ C·m is obtained at the wavelength of 1537 nm and magnetic field of 0.2 T. Our results could pave the way for realizing solid-state quantum networks at telecom-C band.

Keywords quantum memory, erbium-doped fiber, coherent interaction, transition dipole moment, sub 10 mK

Citation Xi Q, Wei S H, Yuan C Z, et al. Experimental observation of coherent interaction between laser and erbium ions ensemble doped in fiber at sub 10 mK. *Sci China Inf Sci*, 2020, 63(8): 180505, <https://doi.org/10.1007/s11432-020-2954-5>

1 Introduction

Solid-state materials doping with rare-earth ions have attracted growing interests in quantum information applications, especially for solid-state photonics quantum memory [1–3], whose development requires a material with excellent optical or spin coherence properties [4–6]. To that end, rare-earth ions in solid-state materials below <4 K are strong candidates because of their narrow homogeneous linewidth, long coherence time, and large inhomogeneous broadening [7–11]. The erbium ion has the $^4I_{15/2}$ - $^4I_{13/2}$ transition in telecom C-band wavelength-compatible with fiber communication systems [12, 13], and can

* Corresponding author (email: hzsong1296@163.com, gw deng@uestc.edu.cn, zhouqiang@uestc.edu.cn)

provide high optical depth inside the fiber core for efficient photon-atom interaction, making it practical for photonics quantum information applications [14]. For these applications, the coherent interaction between erbium ions and photons are crucial and must be investigated. McAuslan *et al.* [15] obtained the ${}^4I_{15/2}$ - ${}^4I_{13/2}$ transition dipole moment μ of 3.5×10^{-32} C·m in Er^{3+} : LiNbO_3 . Hiraishi *et al.* [16] measured a transition dipole moment μ of 7.6×10^{-32} C·m in ${}^{167}\text{Er}^{3+}$: Y_2SiO_5 with a 10 ppm atomic concentration of ${}^{167}\text{Er}^{3+}$ at a temperature of 2.2 K via Rabi oscillation. However, the coherent interaction between light and erbium ions doped in optical fibers have not yet been studied at or below 10 mK. At this temperature, the optical and spin coherence times are expected to be substantially improved, due to the decreased phonon density in the Er^{3+} -doped fiber with lower temperature [17].

In this study, we have investigated the coherent interaction between laser and erbium ions doped in a 9.5 m long piece of fiber at a temperature of 7 mK in a cryogenic dilution refrigerator (LD400, BlueFors). We measured the coherent optical nutation on the ${}^4I_{15/2}$ - ${}^4I_{13/2}$ transition and thus extracted the transition dipole moment. Interesting excitation transition wavelength and magnetic field dependences of the transition dipole moment were also revealed in our measurement and the possible explanations related to inhomogeneous broadening of optical transition have been given. Our results pave a potential path for developing solid-state photonics quantum memory and quantum networks based on Er^{3+} -doped fibers.

2 Experimental setups

Figure 1 shows the experimental setup for cooling down the Er^{3+} -doped silica fiber to ultra-low temperatures using a dilution refrigerator. Our experiments employ a sample of 9.5-m-long Er^{3+} -doped fiber (INO Canada, S/N 402-28254), co-doped with 200 ppm-wt Er, 1.0 wt% Al, and 7.9 wt% Ge. Two single-mode bare fibers, which are used for applying input laser and collecting output signals, are connected with the Er^{3+} -doped fiber, as shown in Figure 1(a). To obtain good thermal contact, these bare fibers are fixed with adhesive tape on each cold plate inside the dilution refrigerator. The sample holder is shown in Figure 1(b), which shows the Er^{3+} -doped fiber wound around a copper cylinder with a diameter of 3.4 cm. Each port of Er^{3+} -doped fiber is directly fusion spliced with a single-mode fiber. A copper plate with dimensions of 18 mm×452 mm×2 mm is designed to hold the fiber sample lying between the mixing chamber flange and magnet. Our sample can be cooled down to a temperature of 7 mK—the cooling effect mainly depends on the heat of mixing of He3 and He4 [18,19]. Moreover, a superconducting magnet with magnetic field of up to 7 T is mounted in our dilution refrigerator.

The experimental schematic is illustrated in Figure 1(c). Continuous-wave laser light is generated by an external-cavity diode laser whose linewidth is around 10 kHz and wavelength can be tuned from 1528 to 1566 nm. The laser beam is then temporally shaped into pulses by using a 200 MHz acousto-optic modulator (AOM) with an extinction ratio of 60 dB. The laser pulses have duration of 500 ns and repetition rate of 20 Hz. This configuration can guarantee that the erbium ions excited by one pulse can completely decay to their ground states when the next pulse reaches them. The AOM is driven by an arbitrary function generator (AFG). The waveform of the input pulse is monitored before being sent into the dilution refrigerator, using a 95:5 beam splitter and a photodetector (PD1). The peak power of input pulse ranging from 0.71 to 6.05 mW is controlled by employing a variable optical attenuator (VOA1). The transmitted signal through the Er^{3+} -doped fiber is detected by another photodetector (PD2). The output of PD2 is observed with an oscilloscope.

3 Results

Optical depth — defined as αL , where L is the length of the medium, α is the absorption coefficient [20] — is a dimensionless quantity for characterizing the absorption of a medium. By employing amplified spontaneous emission (ASE) light from an Er^{3+} -doped fiber amplifier, we measure the optical depth of the 9.5-m-long Er^{3+} -doped fiber at 7 mK over a broad wavelength range, as shown in Figure 2. The inhomogeneously broadened line results in an optical depth, which distributed over several tens of

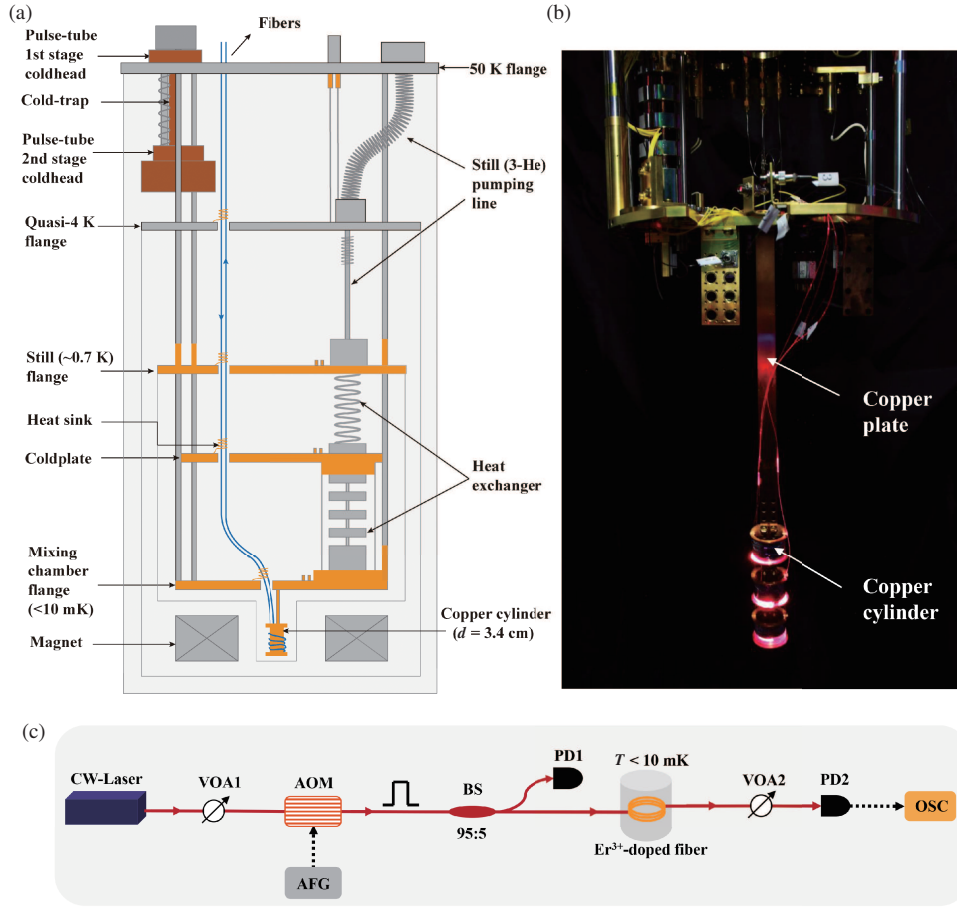


Figure 1 (Color online) (a) Schematics of main components in the dilution refrigerator. It shows the different temperature flanges, including the 50 K flange, quasi-4 K flange, still flange, cold-plate, and mixing chamber flange. The Er³⁺-doped fiber sample is placed in the center of the magnetic coil under the mixing chamber flange. (b) Photograph of the sample holder for Er³⁺-doped fiber. A red light beam is injected into the fiber to coarsely determine whether there is any strongly scattering point along the routine of light. (c) Experimental setup for optical nutation measurements. The laser wavelength is tunable from 1528 to 1537 nm in the experiment. VOA2 (variable optical attenuator2) is used to protect the PD2 from the high peak power; AOM; AFG; BS, 95:5 beam splitter; PD, PD1, and PD2 are connected to ports with low and high beam splitting ratios, respectively; OSC, oscilloscope.

nanometers of wavelength. The absorption peak of our Er³⁺-doped fiber sample lies at 1530 nm at which the optical depth is ~ 3.24 , and the measured optical depths at the wavelengths ranging from 1528 to 1537 nm (1 nm every interval) are 3.14, 3.21, 3.24, 3.21, 3.11, 2.93, 2.65, 2.3, 1.85, and 1.4, respectively.

To explore the coherent interaction between photons and atoms in the Er³⁺-doped fiber, we conduct optical nutation measurements, and calculate the $^4I_{15/2}$ - $^4I_{13/2}$ transition dipole moment μ of erbium ions under the condition of various transition wavelengths and magnetic field strengths. Optical nutation is a phenomenon in which the pulse transmission oscillates in sync with the atomic ground state population. The Rabi frequency can be extracted from optical nutation signal based on the time t , measured from the beginning of the pulse, at which the first nutation signal peak occurs. The relationship can be described by the following equation [21]:

$$\Omega t = 1.635\pi(1 + 0.116\alpha L), \quad (1)$$

where Ω is Rabi frequency and αL is the measured optical depth. The obtained time-dependent decay of optical nutation signals at the wavelength of 1533 nm is shown in Figure 3(a). Note that the actual shape of nutation signals only results in one discernible peak of the oscillation. This is affected by the characteristics of the input pulse and the Er³⁺-doped fiber including the inhomogeneous broadening of an atomic ensemble, the inhomogeneous intensity distribution of the light in guided fiber mode and the

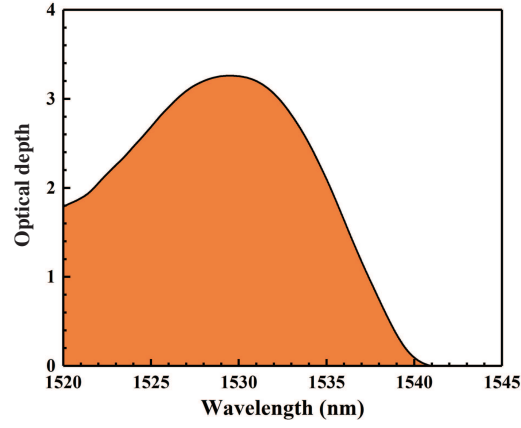


Figure 2 (Color online) Absorption spectrum of the ${}^4I_{15/2}$ - ${}^4I_{13/2}$ transition of Er^{3+} in the 9.5-m-long fiber. The results of optical depth at different wavelengths are used to calculate the transition dipole moment.

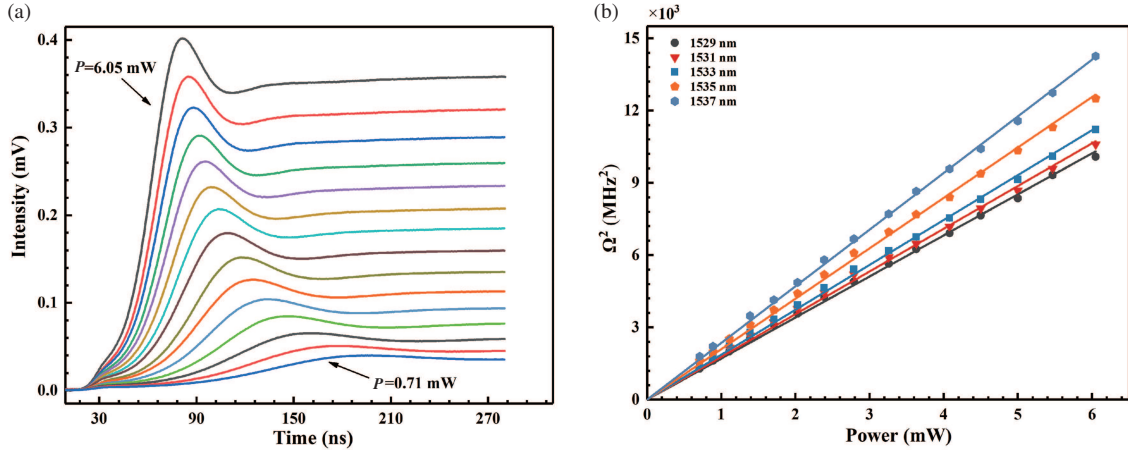


Figure 3 (Color online) (a) The observed optical nutation signals of Er^{3+} -doped fiber at the wavelength of 1533 nm. The excitation pulses of peak power used to calculate Rabi frequency range from 0.71 to 6.05 mW (shown with different colors). (b) The power dependence of Ω^2 . The input laser wavelengths are set at 1529 nm (circle), 1531 nm (triangle), 1533 nm (square), 1535 nm (pentagon), and 1537 nm (hexagon). The solid lines are the result of linear fitting.

homogeneous broadening of atoms [22]. All optical nutation measurements are averaged five times under the same experimental condition, in order to minimize the errors on account of the temporal jitter of laser pulse and other noises, such as the laser power fluctuations, electronic noises in photodetector and oscilloscope.

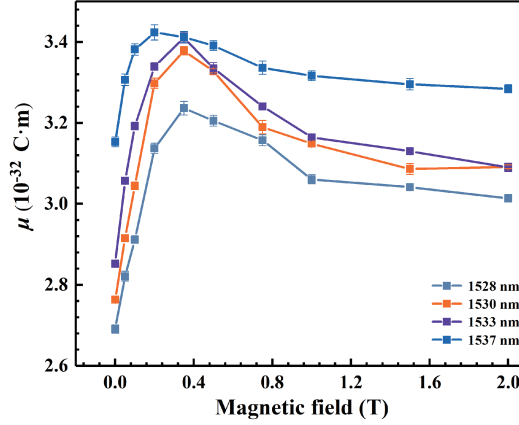
The data in Figure 3(a) shows that the time of the first peak of the nutation signal is inversely proportional to pulse peak power P , which means that the Rabi frequency is positively correlated with P . According to the photon-atom interaction theory in optical waveguide, a linear power dependence of Ω^2 and the ${}^4I_{15/2}$ - ${}^4I_{13/2}$ transition dipole moment μ can be deduced as [23]

$$\Omega^2 = \kappa \frac{\mu^2}{A} P, \quad (2)$$

where P represents the pulse power entering into the sample, A is the mode field area of Er^{3+} -doped fiber and $\kappa = 2(n^2 + 2)^2 / (9nc\varepsilon_0\hbar)$ is a material constant relating local electric field to the optical intensity [24]. The refractive index n of the Er^{3+} -doped fiber is 1.463 and $A \approx 11.9\pi \mu\text{m}^2$. Eq. (2) indicates that μ can be calculated based on the measured power dependence of Ω^2 . In our experiment we record the optical nutation signals when the powers and wavelengths of the input laser are set to different values. By Eq. (1), we extract the Rabi frequency Ω in each signal, and plot the Ω^2 versus P under different input laser wavelengths in Figure 3(b). The corresponding calculated results of the transition dipole moment are

Table 1 Calculated ${}^4I_{15/2}$ - ${}^4I_{13/2}$ transition dipole moments of erbium ions in fiber at various laser wavelengths

Wavelength (nm)	Transition dipole moment (10^{-32} C·m)	Wavelength (nm)	Transition dipole moment (10^{-32} C·m)
1528	2.634 ± 0.009	1533	2.814 ± 0.008
1529	2.691 ± 0.008	1534	2.926 ± 0.006
1530	2.714 ± 0.008	1535	2.983 ± 0.009
1531	2.745 ± 0.010	1536	3.037 ± 0.008
1532	2.794 ± 0.008	1537	3.161 ± 0.007

**Figure 4** (Color online) Dependence of transition dipole moment on magnetic field. Measurements are carried out under different strengths of magnetic field. Various laser wavelengths are in different colors.

demonstrated in Table 1.

In Figure 3(b), the dependence of Ω^2 on P can be fitted well by a linear function for each wavelength, which is consistent with Eq. (2). With the slope of each fitted line in Figure 3 (b) and Eq. (2), the transition dipole moment μ is calculated and shown in Table 1. It is obvious in Table 1 that μ increases with increasing input laser wavelength. This phenomenon is inconsistent with the theoretical model in a few works [25], in which the oscillation strength of the ${}^4I_{15/2}$ - ${}^4I_{13/2}$ transition is considered to be invariant for all the atoms in the sample. However, the wavelength dependence can be understood from the origin of inhomogeneous broadening. It is well known that ${}^4I_{15/2}$ and ${}^4I_{13/2}$ will split into 8 and 7 Stark levels, respectively, after interacting with the crystal-field potential [26]. Since the crystal-field potential changes with local sites, the transition frequencies and dipole moments between the Stark levels are slightly different for Er^{3+} at different spatial sites in an Er^{3+} -doped fiber. Such spatial inhomogeneity, together with the fractions of atoms in different sites, lead to the inhomogeneous broadened absorption profile. An input laser with certain wavelength can excite transitions between Stark levels in atoms within similar environment, and the measured dipole moment μ in such case belongs to the dominant transitions. Thus, different μ will be obtained when the input laser wavelength varies, as shown in Table 1. The same mechanism also leads to the dependence of the transition probability in fluorescence radiation on the radiation wavelength, and has been studied in Nd^{3+} - and Eu^{3+} -doped glass [26].

The magnetic field causes the ground and excited electronic levels to each split into pairs of Zeeman sublevels [27]. In addition to performing optical nutation measurements under various transition wavelengths, we also study the transition dipole moment at different magnetic field strengths. The magnetic field dependence of the ${}^4I_{15/2}$ - ${}^4I_{13/2}$ transition dipole moment of erbium ions in fiber is plotted in Figure 4, with magnetic fields from 0 to 2 T.

As shown in Figure 4, we note that as the strength of the magnetic field increases, the transition dipole moment first increases, then decreases, and finally approaches a constant. This phenomenon appears at all wavelengths but the maximum transition dipole moment happens at different magnetic field strengths. As a result, the largest ${}^4I_{15/2}$ - ${}^4I_{13/2}$ transition dipole moment of erbium ions in the fiber is $(3.424 \pm 0.019) \times 10^{-32}$ C·m, occurring for the wavelength of 1537 nm and the magnetic field of 0.2 T. Compared with the previous results under zero magnetic field, we find that a magnetic field practically

contributes to the transition dipole moment value, but the details of the reason for such phenomena requires further experiments. We can provide one explanation here, by resorting to the inhomogeneous broadening and the Zeeman effect. When the magnetic field is absent, an input laser with λ_i will interact most intensively with atoms for which the ${}^4I_{15/2}$ - ${}^4I_{13/2}$ transition has resonant wavelength of λ_i , and the measured dipole transition is related with these atoms. When magnetic field is turned on, both of the ${}^4I_{15/2}$ and ${}^4I_{13/2}$ will be split into two sublevels by Zeeman effect and therefore four transitions appears in this four-level system [28, 29]. Thus, with the external magnetic present, atoms initially resonant with the input laser will probably get significantly detuned, while other atoms initially not resonant the laser would come into resonance due to the Zeeman shift. When the magnetic field strength increases, the Zeeman splittings in each atom become larger, and atoms corresponding to different positions in the homogeneously broadened absorption spectrum would get resonant to the input laser via Zeeman transition successively [30]. It has been revealed in Figure 3 that these atoms have different transition dipole moment under zero magnetic field. Since the Zeeman sublevels are the results of the perturbation of magnetic field on the ${}^4I_{15/2}$ and ${}^4I_{13/2}$ levels, it is expected that the transition dipole moments of Zeeman transitions in these atoms are also different. Therefore, the measured transition dipole moments under different magnetic field strengths belong to the Zeeman transitions in different atoms along the inhomogeneous broadening absorption spectrum. We can claim that the inhomogeneous broadening and Zeeman effect together lead to the complex dependence of the transition dipole moment on magnetic field and input laser wavelength.

4 Conclusion

In this paper we have measured the optical nutation for characterizing the coherent photon-atom interaction of erbium ions in a fiber cooled to 7 mK for the first time. We further extracted the ${}^4I_{15/2}$ - ${}^4I_{13/2}$ transition dipole moment through nutation signals and obtained a transition dipole moment around 10^{-32} C·m under the conditions of different transition wavelengths and magnetic fields. Our results are consistent with previous ones that extracted from Er^{3+} -doped crystals on the order of magnitude [15, 16]. We observed that the transition dipole moment linearly depends on the transition wavelength of erbium ions. An exotic magnetic field dependence of the transition dipole moment has also been observed in our experiment. However, a completely clean mechanism for such phenomenon has not yet been provided, which should be studied in the future. In summary, our results provide evidences for understanding the coherent interaction between laser and erbium ions at 7 mK and can promote the Er^{3+} -doped fiber to become a promising candidate for solid-state quantum memory.

Acknowledgements This work was supported by National Key R&D Program of China (Grant No. 2018YFA0307400), National Natural Science Foundation of China (Grant Nos. 61775025, 91836102, 61705033, 61405030, 61308041), Alberta Major Innovation Fund and the National Science and Engineering Research Council of Canada (NSERC).

References

- 1 Thiel C W, Böttger T, Cone R L. Rare-earth-doped materials for applications in quantum information storage and signal processing. *J Lumin*, 2011, 131: 353–361
- 2 Sun Y, Thiel C W, Cone R L, et al. Recent progress in developing new rare earth materials for hole burning and coherent transient applications. *J Lumin*, 2002, 98: 281–287
- 3 Lvovsky A I, Sanders B C, Tittel W. Optical quantum memory. *Nat Photon*, 2009, 3: 706–714
- 4 Saglamyurek E, Sinclair N, Jin J, et al. Broadband waveguide quantum memory for entangled photons. *Nature*, 2011, 469: 512–515
- 5 Kunkel N, Goldner P. Recent advances in rare earth doped inorganic crystalline materials for quantum information processing. *Z Anorg Allg Chem*, 2018, 644: 66–76
- 6 Tittel W, Afzelius M, Chanelière T, et al. Photon-echo quantum memory in solid state systems. *Laser Photon Rev*, 2009, 4: 244–267
- 7 de Riedmatten H, Afzelius M, Staudt M U, et al. A solid-state light-matter interface at the single-photon level. *Nature*, 2008, 456: 773–777
- 8 Saglamyurek E, Jin J, Verma V B, et al. Quantum storage of entangled telecom-wavelength photons in an erbium-doped optical fibre. *Nat Photon*, 2015, 9: 83–87

- 9 Veissier L, Falamarzi M, Lutz T, et al. Optical decoherence and spectral diffusion in an erbium-doped silica glass fiber featuring long-lived spin sublevels. *Phys Rev B*, 2016, 94: 195138
- 10 Sinclair N, Saglamyurek E, George M, et al. Spectroscopic investigations of a waveguide for photon-echo quantum memory. *J Lumin*, 2010, 130: 1586–1593
- 11 Hedges M P, Longdell J J, Li Y, et al. Efficient quantum memory for light. *Nature*, 2010, 465: 1052–1056
- 12 Dajczgewand J, Ahlefeldt R, Böttger T, et al. Optical memory bandwidth and multiplexing capacity in the erbium telecommunication window. *New J Phys*, 2015, 17: 023031
- 13 Saglamyurek E, Puigibert M G, Zhou Q, et al. A multiplexed light-matter interface for fibre-based quantum networks. *Nat Commun*, 2016, 7: 11202
- 14 Macfarlane R M, Sun Y, Sellin P B, et al. Optical decoherence times and spectral diffusion in an Er-doped optical fiber measured by two-pulse echoes, stimulated photon echoes, and spectral hole burning. *J Lumin*, 2007, 127: 61–64
- 15 McAuslan D L, Longdell J J, Sellars M J. Strong-coupling cavity QED using rare-earth-metal-ion dopants in monolithic resonators: what you can do with a weak oscillator. *Phys Rev A*, 2009, 80: 062307
- 16 Hiraishi M, IJspeert M, Tawara T, et al. Optical coherent transients in $^{167}\text{Er}^{3+}$ at telecom-band wavelength. *Opt Lett*, 2019, 44: 4933–4936
- 17 Macfarlane R M. High-resolution laser spectroscopy of rare-earth doped insulators: a personal perspective. *J Lumin*, 2002, 100: 1–20
- 18 Wheatley J C, Vilches O E, Abel W R. Principles and methods of dilution refrigeration. *Phys Physique Fizika*, 1968, 4: 1–64
- 19 Uhlig K. $^3\text{He}/^4\text{He}$ dilution refrigerator with pulse-tube refrigerator precooling. *Cryogenics*, 2002, 42: 73–77
- 20 Afzelius M, Simon C, de Riedmatten H, et al. Multimode quantum memory based on atomic frequency combs. *Phys Rev A*, 2009, 79: 052329
- 21 Vega D S, Rambow P B, Tian M Z. Optical nutation in an optically thick and inhomogeneously broadened atomic ensemble. *J Opt Soc Am B*, 2018, 35: 1374–1378
- 22 Sun Y, Wang G M, Cone R L, et al. Symmetry considerations regarding light propagation and light polarization for coherent interactions with ions in crystals. *Phys Rev B*, 2000, 62: 15443–15451
- 23 Sinclair N, Oblak D, Thiel C W, et al. Properties of a rare-earth-ion-doped waveguide at sub-kelvin temperatures for quantum signal processing. *Phys Rev Lett*, 2017, 118: 100504
- 24 Thiel C W, Macfarlane R M, Sun Y, et al. Measuring and analyzing excitation-induced decoherence in rare-earth-doped optical materials. *Laser Phys*, 2014, 24: 106002
- 25 Hilborn R C. Einstein coefficients, cross sections, f values, dipole moments, and all that. *Am J Phys*, 1982, 50: 982–986
- 26 Brecher C, Riseberg L A, Weber M J. Variations in the transition probabilities and quantum efficiency of Nd^{3+} ions in ED-2 laser glass. *Appl Phys Lett*, 1977, 30: 475–478
- 27 Saglamyurek E, Lutz T, Veissier L, et al. Efficient and long-lived Zeeman-sublevel atomic population storage in an erbium-doped glass fiber. *Phys Rev B*, 2015, 92: 241111
- 28 Guillot-Noël O, Goldner P, Antic-Fidancev E, et al. Analysis of magnetic interactions in rare-earth-doped crystals for quantum manipulation. *Phys Rev B*, 2005, 71: 174409
- 29 Louchet A, Habib J S, Crozatier V, et al. Branching ratio measurement of a Tm^{3+} : YAG system under a magnetic field. *Phys Rev B*, 2007, 75: 035131
- 30 Liu G, Be'er O, Margalit Y, et al. Survival of the fittest in the coherent evolution of quantum ensembles. *Phys Rev A*, 2018, 98: 013856